Earthquake Engineering, Tenth World Conference © 1992 Balkema, Rotterdam. ISBN 90 5410 060 5

Local buckling and structural damage in steel members under cyclic loading

C.A.Castiglioni & P.L.Losa
Dipartimento di Ingegneria Strutturale, Politecnico di Milano, Italy

ABSTRACT: Typical results representative of a number of experimental tests performed by the authors imposing cyclic displacements at the top of full scale cantilever steel specimens built by HEA and HEB profiles are presented and discussed with regard to structural damage accumulation.

1 INTRODUCTION

At the Structural Engineering Department of Politecnico di Milano, Italy, an experimental testing program is being carried out that encompasses cyclic quasi-static tests to be performed on 45 full scale rolled steel beams of the commercial shapes HE220A, HE220B and IPE300 (15 tests for each type).
Two different testing procedures are followed:

1. quasi-static tests with imposed displacement cycles of constant amplitude Δv;
2. quasi-static tests with imposed displacements following a "random" path, previously obtained by dynamic numerical simulation of the seismic response of similar elements (Ballio et al., 1988).

Research in the field of seismic and cyclic behavior of steel structures has been widely performed, both experimentally and numerically, by the Steel Construction Group of the Structural Engineering Department of Politecnico di Milano (see Seismic Design of Steel Structures, 1990).
During some of these previous research works, experimental data were obtained and numerical simulation models developed and calibrated. In particular, a model was developed by Castiglioni & DiPalma (1988), enabling a fair good correlation between experimental results and numerical simulation. The model, accounting for structural damage due to both local buckling and low cycle fatigue, was calibrated on a small number of tests carried out following the ECCS Recommended Testing Procedures (1986). According to these Recommendations, groups of three displacement cycles are imposed to the specimen, each group having an increased cycle amplitude. These loading procedure, although allowing a correct assessment of the global behavior of the specimen under testing, are not suitable for the assessment of the single aspects, governing such behavior. In fact, by varying the amplitude of the displacement cycles, strain hardening effects are superimposed to reductions in load carrying capacity due to local buckling and low cycle fatigue crack propagation.
For this reason, the present research focused on constant amplitude testing, as other authors (Krawinkler et al.,1983) previously suggested.
Objectives of the research are:

1. collection of a larger number of information than previously available, by means 15 displacement transducers applied to the specimens in the plastic hinge zone. These instruments, connected to a computer, allowed a continuous monitoring of local buckling and accumulation of damage during the tests.
2. improvement of the calibration of the numerical model by Castiglioni and DiPalma, on the new experimental results.
3. experimental assessment of the collapse criteria and of the cumulative damage model proposed by Castiglioni and Goss, 1989.

The research is currently under completion. In this paper some typical results are presented and discussed, with reference to a rapresentative test performed on a HE220A member. Detailed results of the whole experimental research are presented elsewhere by Castiglioni & Losa (1992).

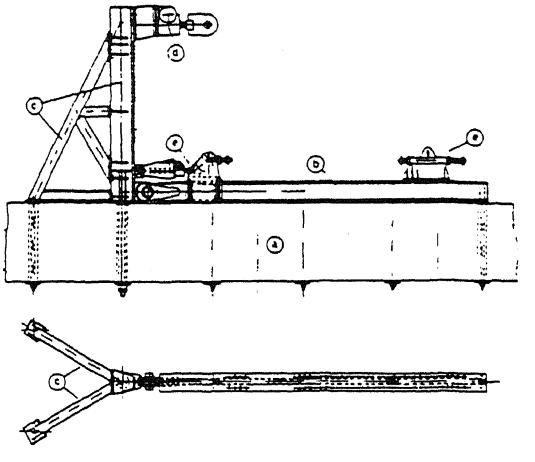

fig. 1 Testing equipment

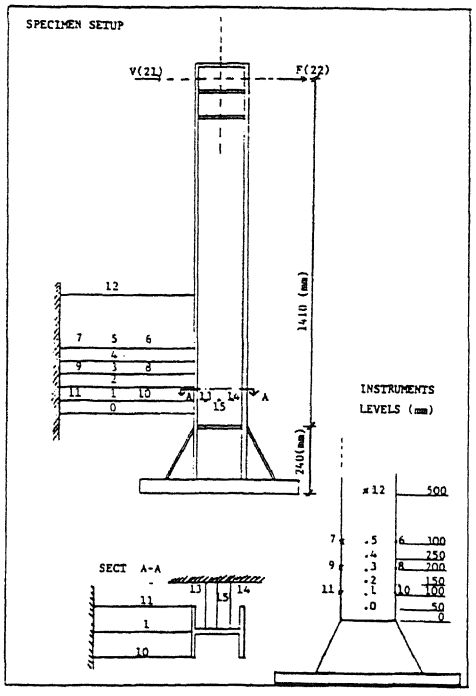

fig. 2 Specimen setup

Tab. 1 - Table 1

Profilo (Shape)	Area (Area) (cm²)	Ala (Flange)			Anima (Web)		
		b	t	b/t	h	t_w	h/t_w
HE 220A	64.3	220	11.0	20.0	188.0	7.0	26.8
HE 220B	91.0	220	16.0	13.8	188.0	9.5	19.8
IPE 300	53.8	150	10.7	14.0	278.6	7.1	39.2

2 THE EXPERIMENTAL RESEARCH

2.1 Test setup

Tests were performed using the equipment designed by Ballio & Zandonini (1985), that is capable of applying horizontal cyclic actions in a quasi-static way. The possible specimen size is approximately 3.0 m. Forces (F) and displacements (v) range between ±1000 KN and ±300 mm. A power jackscrew enables displacements to be assumed as control parameters and, consequently the unstable branch of the specimen's behavior to be followed (fig. 1). The testing equipment main components are :

a) foundation (fig. 1.a)
b) supporting girder (fig. 1.b)
c) counterframe (fig. 1.c)
d) main jack (fig. 1.d)
e) axial loading system (fig. 1.e)

In order to evaluate the behavior of the specimen in the plastic hinge zone, in addition to the top displacement and applied force, a number of displacement transducer were connected to the web and the flanges of the specimen (fig. 2). The instruments on the specimen flanges are applied, on different levels, at various distance from the base, both at center, near the web to flange connection, to obtain informations on plastic rotations and curvature at the plastic hinge, and at the edges, in order to obtain information regarding torsion and local buckling of the flange plates. Connection of these instruments was carefully realized, in order to avoid measurements of undesirable displacement components.

The instruments connected to the specimen web were placed at the same level as those on the flanges, allowing the assessment of the web buckling and its correlation with that of the flange plates.

The specimens dimensions are shown in fig. 2, while the properties of the profiles are given in tab.1.

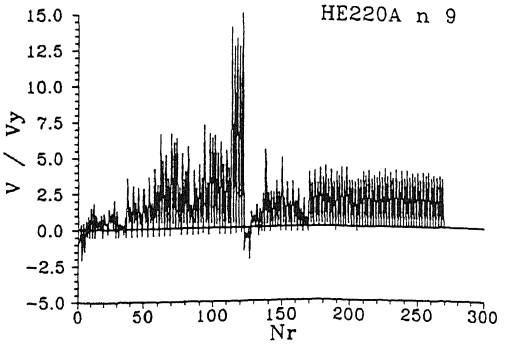

fig. 3 Random loading history for HEA n.9 test

2.2 Testing program

Presently 24 tests were already performed (11 HE220A and 13 HE220B). Of these, 8 HE220A and 9 HE220B were performed imposing to the specimens displacement cycles with a constant amplitude (Δv) and zero mean value (v_m).

Furthermore, in order to assess the seismic behavior of these members and the validity of the damage accumulation model presented by Castiglioni & Goss (1989), some random displacement histories were numerically obtained by means of the dynamic numerical simulation code presented by Ballio, Castiglioni & Perotti (1988). This model, set up in order to simulate the dynamic behavior of columns under compression and bending, consists of a rigid bar connected to the ground by a "cell" where all the deformability of the member is concentrated and a structural lumped mass applied on the top. The behavior of the "cell" follows a constitutive law for the material and accounts for damage, according to the rules and the model proposed by Castiglioni & DiPalma (1988). The oscillograms numerically obtained as output from the dynamic simulation (fig. 3) were imposed in a quasi-static way to the specimens under testing. To date 4 HE220A and 3 HE220B beams were tested under random cycles.

3 EXPERIMENTAL RESULTS

3.1 Description of typical results

Here typical results of a cyclic test are presented, with regard to a HE220A beam subjected to displacement cycles having a constant amplitude Δv= 120 mm. For the

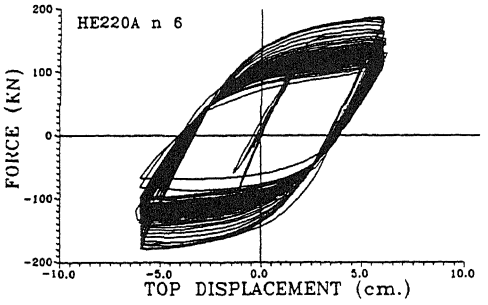

fig.4 Typical load-deflection diagram

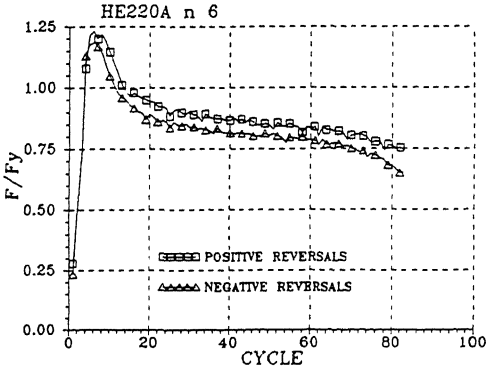

fig. 5 Typical reduction trend of load carrying capacity

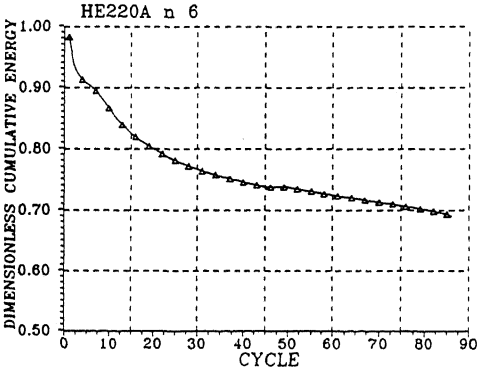

fig. 6 typical trend of cumulative energy

specimen under testing this corresponds to a ductility demand $\Delta v/v_y = 5.71$, where v_y is the yield displacement, determinated according to ECCS (1986).

Fig. 4 shows the response of the specimen in terms of force applied on the top vs. top displacement. It can be noticed how, after the first cycles, applied in the elastic range, when the first cycle in the plastic range is imposed, strain hardening effects generate an increase in the loadd carrying capacity of the beam. After nearly five cycles a reduction in strength takes place, because of local buckling of the flange plates. This is clearly evident also by examining fig. 5, where the load carrying capacity (F) of

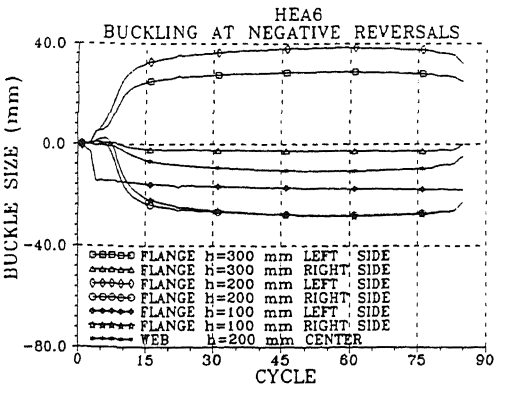

fig. 7 Typical trend of buckle size

the specimen at each reversal is plotted against the number of imposed cycles, normalized on the yield strength (F_y), determinated according to ECCS (1986). From fig. 5 it becomes also evident how, after an initial loss in carrying capacity with a rather high gradient, beyond the 20th cycle a stabilization of the behavior takes place and the rate of deterioration is greatly reduced, up to the last cycles before complete failure (say until the 75th cycle) when a further increase can be noticed.

This behavior is furtherly explained by examining figs. 6 and 7. In fig. 6 the absorbed cumulative energy (defined as the sum of the areas of all the cycles imposed to the specimen) is plotted versus the number of cycles, normalized by corresponding one for an ideal specimen made of an elastic perfectly plastic material.

Fig.7 shows the buckle size of the flange edges (i.e. the maximum deflection of the flange due to buckling), vs. the number of cycles.

After local buckling takes place, the out-of-plane displacements of the flange-edges suddendly increase for several cycles, and then the rate of growth decreases steadly until a stage of stabilization is reached.

It is then clear how and why the effects of local buckling on the load deflection response (fig. 4) is a continuous decrease in strength (fig.5), stiffness and hysteresis loop area (fig. 6).

The following fig. 8 shows the torsion of the flange, at 10 cm. from the specimen base, plotted vs. the axial force in the flange, evaluated dividing the applied bending moment by the distance between the centers of gravity of the flange plates. It can be observed that after some cycles characterized by very small plastic deformations, large permanent distorsions occur (due to flange buckling), whose rate of growth steadily decreases. After a few cycles, stable loops around the permanently displaced position take place. It is also evident that the load carrying capacity of the beam decreases steadily, as shown by the fairly constant rate of reduction of the axial force in the flange, while the displacement cycles imposed to the specimens have of the same amplitude. This means that, increasing the number of cycles imposed to the specimen, the force applied by the jack to impose the same, required, displacement is steadily reduced.

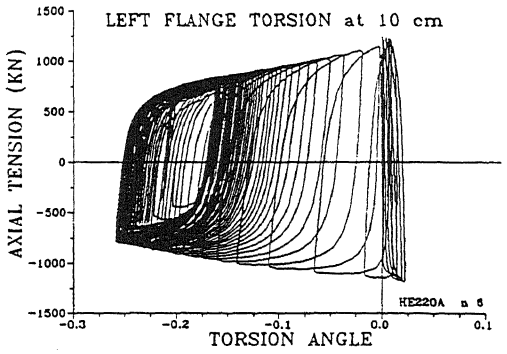

fig. 8 Typical axial load - torsion angle diagram

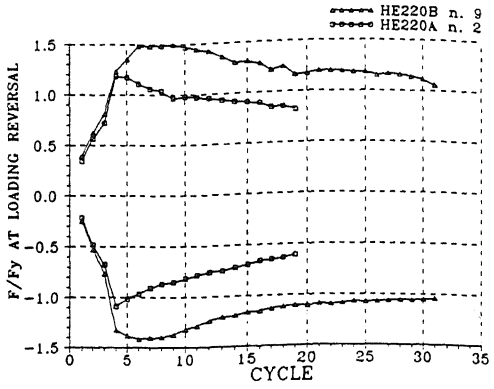

fig. 9 HEA and HEB strength deterioration trends

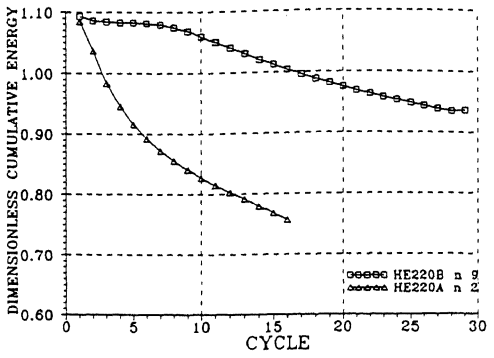

fig. 10 HEA and HEB absorbed energy trends

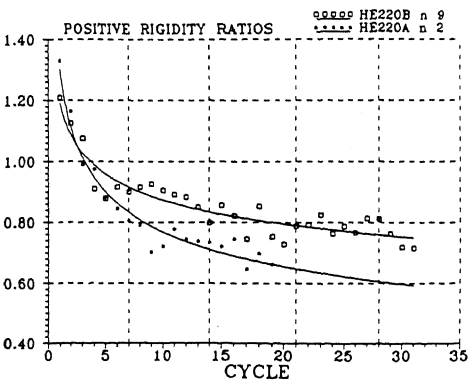

fig. 11 HEA and HEB stiffness deterioration trends

3.2 Comparison between HEA and HEB beams behavior

From the experimental results optained to date, some general remarks can be stated, regarding the differences in behavior of two types of profiles. This will be done hereafter, with reference to two typical tests, one regarding HE220A profiles (HEA n.2, carried out with a Δv=240 mm, $\Delta v/v_y$=12) and one regarding HE220B profiles (HEB n.9, with Δv=200 mm and $\Delta v/v_y$=11.1). Before any comment it is however important to highlight the fact that HE220B profiles are characterized by width to thickness ratios of both the web and the flange plates much lower than the HE220A (tab.1).
The comparison of the different behaviors is carried out in the following fig. 9-11, which respectevely show that:

1. Strain hardening effects are much greater in HEB rather than in HEA beams (fig. 9);

2. Deterioration effects, causing a reduction in the load carrying capacity (fig. 9), hysteresis loops area (fig.10) and stiffness (fig. 11), begin earlier in HEA beams (having larger width to thickness ratios) rather than in HEB ones; Fig. 11 plots the reduction of the rigidity ratio (defined as the tangent modulus corresponding to the change of the sign of the applied load, normalized by the initial elastic one) vs. the number of applied cycles.

3. Once local buckling took place, the hysteresis loops stabilize, and the rate of reduction in load carrying capacity decreases with increasing the number of cycles imposed to the specimen. This effect is common to both profile types;

4. Corresponding to the last load reversal before failure, the load carrying capacity of the specimen is nearly 70% of the yield strength for HEA beams, while nearly 100% for HEB beams (fig. 9). This is due to the large strain hardening which is typical of HEB beams, that in the first cycles show an increase of the load carrying capacity of more than 10% of the yield strength;

5. The two profiles showed different failure modes, the HEA by steady crack propagation due to low-cycle fatigue effects, the HEB by some kind of brittle fracture, of both flange and web, either at specimen-to-base welds or at plastic hinge, where, due to the large localized distorsions, surface cracks usually develop a few cycles after local buckling of the flange plates.

3.3 Random loading tests

Fig. 12 shows the load deflection curve for one of the random loading tests performed, (test HEA n. 10).
The oscillogram imposed to the specimen is presented in fig. 13, where the ductility demand (defined as the maximum imposed displacement v, normalized by the yield displacement v_y) is plotted vs. the number of load reversals N_r.
Examining fig. 12, it can be noticed that, after some cycles, characterized by small plastic deformations, at nearly the 150th load reversal, some very large plastic

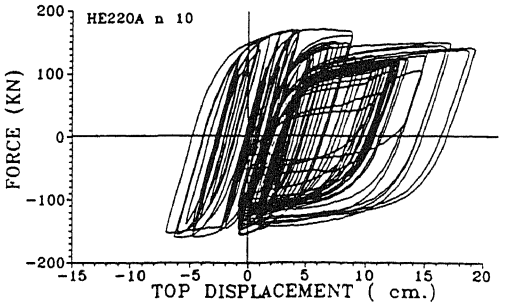

fig. 12 load-deflection diagram for random loading test

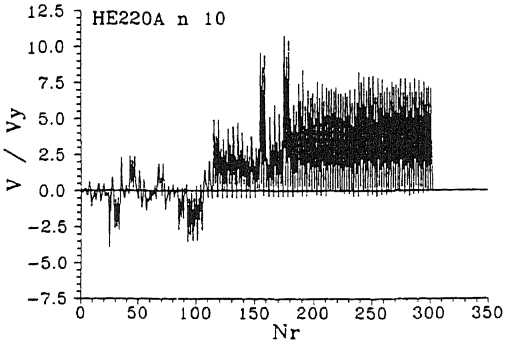

fig. 13 Random loading history for HEA n. 10 test

deformations are imposed to the specimen.
These result in an evident reduction of the load carrying capacity of the beam due to buckling of the flange plates. By continuing cycling, the strength of the specimen is steadily reduced until, in the last cycles, crack propagation occured and caused complete fracture of the flange and part of the web plates.

4 CONCLUSION

From the carried out tests it has been possible to obtain for both HEA and HEB beams the relationships between cycle amplitude Δv and the number of cycles to failure N, which are presented in the following figs. 14 and 15, plotted in a log-log scale.
It can be noticed that for both profiles the $\Delta v/v_y$-N relationship can be fitted by means of an exponential function of the type $N = a \cdot (\Delta v/v_y)^b$, with a and b constant parameters, to be defined and calibrated on the experimental test results, for the different types of profiles. In a log-log scale, such an equation plots as a straight line. The equation of such line is given in the same figures. This is in good agreement with previous experimental results by Krawinkler et al. (1983) and with the Coffin (1954) and Manson (1953) findings.
As can be noticed by examining figs. 14 and 15, the interpolation of HE220A test data is better than that for HE220B. This is due to the different failure mode, already discussed; some HE220B specimens, in fact, failed by fracture at the base welds.
These $\Delta v/v_y$-N relationship are used, as it will be shown elsewere (Castiglioni&Losa, 1992) to assess the structural damage in beams under random loading.

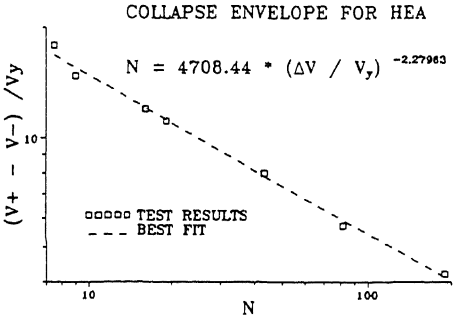

fig. 14 Cycle amplitude - life for HE220A

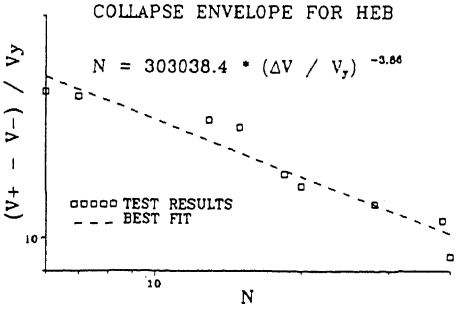

fig. 15 Cycle amplitude - life for HE220B

5. REFERENCES

Ballio, G. Castiglioni, C.A. & Perotti, F. 1988. On the assessment of structural design factors for steel structures. IX WCEE, Tokyo, Vol.5

Seismic Design of Steel Structures, 1990, Selected Papers 1985-1989, by Researchers of the Steel Construction Group, Structural Engineering Dept., Politecnico di Milano.

Castiglioni, C.A. & DiPalma, N. 1988. Steel Members under cyclic loads: numerical modelling and experimental verifications. Costruzioni metalliche, n.6.

ECCS (European Convention for Constructional Steelwork), 1986., Recommended Testing Procedure for Assessing the Behavior of Structural Steel Elements under Cyclic Loads. Techn. Publ. n. 45

Krawinkler, H. et. al., 1983. Recommendations for experimental studies on the seismic behavior of steel components and materials. The John Blume earthquake engineering Center, STanford, CA, Rept. 61

Castiglioni, C.A. & Goss, G., 1989. Adopting Miner's rule in low cycle fatigue. Techn. Rept. 8/89. Structural Eng. Dept., Politecnico di Milano, (in italian).

Castiglioni, C.A. & Losa, P.L., 1992, Experimental assessment of the adoption of a linear cumulative damage model for steel members under seismic loading, Techn. Rept. 1/92, Struct. Eng. Dept., Politecnico di Milano, (in italian).

Ballio, G. & Zandonini, R. , 1985. An experimental equipment to test steel structural members and

subassemblages subject to cyclic loads. Ingegneria Sismica, n.2.

Coffin, L.F., 1954. A study of the effects of cyclic thermal stresses on a ductile method. Trans. ASME, Vol. 76

Manson, S.S., 1953. Behavior of materials under conditions of thermal stress. Heat transfer Symp., NACA TN 2933.